PROBABILISTIC ESTIMATION OF REENTRY DEBRIS AREA

Michael A. Weaver[(1)], Richard L. Baker[(1)], Michael V. Frank[(2)]

[(1)]The Aerospace Corporation, PO Box 92957 M4-964, Los Angeles, CA 90009-2957, USA
[(2)]Safety Factor Associates, Inc., 1410 Vanessa Circle, Suite 16, Encinitas, CA 92024, USA

ABSTRACT

A new method is proposed for probabilistically describing the breakup of reentering space debris. The method provides distributions of breakup altitude, debris area, and casualty area. The process begins with discretization of a reentering body into elements, corresponding largely to body components. Through reentry-heating solutions and applied uncertainties of parameters, probabilities for element separation from the parent body are obtained as a function of altitude, while accounting for ablation and fragmentation. Through additional heating and probabilistic analyses, the population of total fragments is reduced to account for fragments not surviving to ground impact. This leaves surviving-debris-area distributions along the reentry trajectory, which can be directly converted to casualty-area distributions. Finally, through a probabilistic aggregation operation, the casualty-area distributions over altitude are converted to a total-casualty-area distribution. Implementation of this new method is demonstrated for several components of a Delta II 2nd stage rocket body.

1. INTRODUCTION

The risk posed by reentering debris, whether from rocket bodies or spacecraft, has traditionally been couched in terms of expected casualties from a specific reentry event. Typically, the areas of fragments surviving reentry are estimated and converted to a total casualty area [1, 2]. Casualty expectation can then be estimated by applying the casualty area to the population distribution over the estimated impact area of the debris. For a random reentry the impact area is confined only by the orbital inclination of the parent body, while for a targeted reentry the impact area lies within a more well-defined debris footprint.

Current methods for obtaining fragment areas rely on deterministic prediction of body response, sometimes combined with specification of an *a priori* breakup altitude [3, 4, 5, 6]. Assumptions are used to compensate for the very large uncertainties in both the models and model parameters. This approach fails to account for the inherently stochastic nature of the reentry process. For example, the nature of how a reentering body disassembles is not well known. The altitude range of breakup, the size, shape, and attitude of fragments, their trajectories and ablation characteristics may all only be approximated using many simplifying assumptions. The use of pre-defined assumptions masks the inherent uncertainties.

The basis of this present work is a relatively simple physical-thermal model for the prediction of casualty area that explicitly addresses the major state-of-knowledge uncertainties and stochastic variability of phenomena. The approach described here (Section 2) is proposed as a counterpoint to the highly complex and detailed deterministic approach represented, for example, in [3]. A method based on simple equations, which also accounts for uncertainties, allows for an investigation of the effects of such uncertainties on the quality of results, and demonstrates the variation in results associated with the uncertainties. Therefore, even relatively simple equations, when used in a way that includes uncertainties, may provide insights into the effect of uncertain parameters and stochastic variables more clearly than a detailed deterministic model. The resulting insights might then point the way toward areas of research that will ultimately improve the accuracy of prediction.

2. DESCRIPTION OF THE APPROACH

In essence, the approach attempts to replace assumptions with probability distributions that represent the range of knowledge and the inherent stochastic variability of the relevant phenomena. In this manner, the uncertainty in the range of possible casualty areas for a spacecraft consistent with current knowledge is revealed.

Simplified physical models are utilized to highlight the probabilistic aspects of the methodology. Reentry trajectories are described by the equations of particle motion over a spherical, non-rotating planet. A lumped-mass body temperature model provides for reentry heating.

2.1 Reentry Trajectory Model

Using initial conditions for velocity vector and altitude from an orbital decay solution, the reentry trajectory is described by Eqs. 1–4:

$$\dot{V} = -\frac{\rho V^2}{2\beta} - g\sin\gamma \quad (1)$$

$$\dot{\gamma} = \frac{g\cos\gamma}{V}\left[\frac{V^2}{g(R_E + z)} - 1\right] \quad (2)$$

$$\dot{z} = V\sin\gamma \quad (3)$$

$$\rho = \rho_0 e^{-z/\alpha} \quad (4)$$

where,

g = gravitational acceleration
R_E = planetary radius
V = velocity magnitude
z = altitude
α = scale height
β = ballistic coefficient (mass/area)
γ = flight-path angle
ρ = atmospheric density
ρ_0 = reference density

2.2 Reentry Heating and Breakup Model

Temperature change for a lumped-mass node with convective heating and radiative cooling is governed by:

$$\dot{T} = \frac{A}{mc_p}\left[Sh(T_0 - T) - \varepsilon\sigma T^4\right] \quad (5)$$

where,

A = heating (wetted) area
S = averaging factor ($0 < S \leq 1$)
c_p = specific heat
h = heat transfer coefficient
m = body mass
T = lump temperature
T_0 = air total temperature
ε = emissivity
σ = Stefan-Boltzmann constant

The averaging factor S is a function of geometry, attitude, and shielding. The effects of geometry and attitude are determined according to methods in [7, 8]. The heat transfer coefficient for the convection term is derived from the Detra-Kemp-Riddell correlation [9, 10] for hypersonic flow:

$$h = \frac{D}{(T_0 - 300\text{K})}\sqrt{\frac{0.3048}{R}}\left(\frac{\rho}{1.225}\right)^{0.5}\left(\frac{V}{7924.8}\right)^{3.15} \quad (6)$$

where,

D = 199.87 MW/m^2
R = heating radius (m)
T_0 = air stagnation temperature (K)
V = freestream velocity magnitude (m/s)
ρ = freestream density (kg/m^3)

Once the node temperature T reaches the material melt temperature T_m, mass loss dM is determined by the material heat of fusion h_{if} according to Eqs. 7 and 8:

$$\frac{\delta Q}{dt} = A\left[Sh(T_0 - T_m) - \varepsilon\sigma T_m^4\right] \quad (7)$$

$$dM = -\frac{\delta Q}{h_{if}} \leq 0 \quad (8)$$

The overall approach applies the breakup criterion that each element separates from the spacecraft when its melting temperature is reached by aerothermal heating (the terms *breakup* and *separation* will be used interchangeably). Therefore, spacecraft breakup in the atmosphere is typically initiated when the lowest melting point material (typically aluminum) is heated to its melt temperature. This may be thought of as mechanical failure due to severely diminished strength modulus at the melt temperature. A more physically realistic extension of this concept in which the failure is based on the allowable stress and strain in the element has previously been developed [11], but has not been applied in this current work. *Demise* of a separated element is defined as complete melting or ablation with no surviving fragments.

2.3 Probabilistic Algorithm

Of primary interest are the projected range of areas that surviving fragments from randomly reentering spacecraft might have as they hit the ground. In such a predictive approach, not only the natural variability of the processes involved in breakup and demise should be included, but also uncertainty in the current level of knowledge about the processes. Observations of reentries indicate that breakup of a spacecraft and its elements is far from instantaneous and the details are not easily predicted. Indeed, the guiding principle behind this current work is that very little is precisely predictable with respect to spacecraft breakup. Elements separate from the main spacecraft, creating a debris train over an extended range of altitudes, perhaps as large as 40 km. The elements that separate may fragment. Elements or their fragments may ablate partially or completely before reaching the ground. An algorithm accounting for these occurrences is next described.

Step 1: Discretize the Spacecraft
An idealized spacecraft is created using elementary geometric surfaces and volumes (cones, cylinders, spheres, plates, rods, etc.). Each element has specific dimensions, and material-related thermal and physical

properties. The choice of idealized geometry may arise naturally from the actual component, e.g., discretizing a spherical pressure tank as a single sphere. However, it may also be convenient to model a component as a collection of smaller elements, e.g., discretizing a frustum-shaped skirt into several trapezoidal plates. In general, discretized elements should be chosen to maintain the approximate thermal and aerodynamic scales of the actual component.

Step 2: Determine Sensitive Parameters

Sensitivity calculations are performed for the parameters in Eqs. 1–8. It was determined that the following parameters are highly uncertain and the results are quite sensitive to their values: averaging factor S, convective heat transfer coefficient h, and emissivity ε. Although uncertain, reasonable upper bounds, lower bounds and central tendencies can be estimated from the characteristics of assumed spacecraft elements. From these, probability distributions may be defined for each sensitive parameter.

Step 3: Simulate to Obtain Probability of Breakup

Starting with incoming spacecraft initial conditions (i.e., velocity and altitude), uncertainty in the parameters within Eqs. 1–8 produces a range of possible breakup altitudes for spacecraft elements. Solving these equations with Latin Hypercube sampling of the uncertain parameters probabilistically develops this range. Each trial selects a set of values from the uncertain parameters and solves Eqs. 1–8 as a function of time. In effect, thousands of reentries are simulated, each with different parameter values in order to understand the range of altitudes of element separation that might occur owing to the variability (and state-of-knowledge uncertainty) of the parameters S, h, and ε. Thus, each element e of a spacecraft is associated with a probability of separation at each altitude j that is denoted by $p_{e,j}^{sep}$.

Step 4: Element Demise or Survival

After element separation is established, the trajectory calculation is reinitialized because the separated element has different characteristics than when attached to the spacecraft. The new initial conditions are the velocity vector, altitude, and temperature at element separation, along with new values for averaging factor, heat transfer coefficient, and ballistic coefficient. The simulation includes ablation for each element resulting from each postulated altitude of separation from the spacecraft. The fraction ablated of each element at ground impact is recorded. Element-altitude pairs (e, j) that exhibit demise (100% ablation) do not contribute to the cumulative area of surviving fragments and need not be carried further in the calculation.

Step 5: Element Fragmentation

Elements may also fragment into smaller pieces. The number of fragments and the area of each may be treated as a random variable in that different reentries would be expected to produce different fragments of the same element. The lower bound for number of fragments an element can break into and still survive to hit the ground is one (i.e., the fragment is the original element). The upper bound may be estimated as a function of the recorded percentage of ablation from Step 4 for each element-altitude pair. Suppose that Δ% of an element had ablated. For small mass increment δ, and all else remaining equal, this implies that it would be possible for fragments of $(\Delta + \delta)$% of the total mass of the original element to have survived. There could be as many as $(100/\Delta - 1)$ of these fragments. This is not a rigorous upper estimate, however the current intention is only to provide for the possibility of fragmentation. A fragment area (the largest-area orientation, neglecting ablation) is determined for each of k possible fragments of an element-altitude pair (e, j). A probability of existence of each possible number of fragments of each element-altitude pair $p_{e,j,k}^{frag}$ is then assigned using a hyper-geometric distribution. Again, the hyper-geometric distribution is a place holder for future development.

Step 6: Fragment Demise or Survival

Having determined the widest range of fragments from each element-altitude pair that might survive to ground impact, it is next determined if each fragment size within the range indeed does survive. Eqs. 1–8 are again applied using initial conditions that correspond to element conditions at the time and altitude of separation from the reentering spacecraft. That is, fragmentation of an element is assumed to occur at the element separation altitude. The size and projected area $A_{e,j,k}^{frag}$ at ground impact of each potential surviving fragment of each element-altitude pair is determined. Because each original fragment area was associated with a probability of existence $p_{e,j,k}^{frag}$, a probability distribution now exists over surviving fragment sizes for each element-altitude pair.

Step 7: Fragment Casualty Area

Each surviving fragment area is augmented to become casualty area by using a standard formulation [e.g., 1, 2] that adds a radius of a person to the radius of an incoming fragment. There obtains,

$$A_{e,j,k}^{c} = \pi\left(R + \sqrt{\frac{A_{e,j,k}^{frag}}{\pi}}\right)^2 \tag{9}$$

where,

$A^c_{e,j,k}$ = casualty area of k^{th} fragment of e^{th} element from separation altitude j, as the fragment impacts earth

R = augmentation radius associated with the union of areas of people with fragments

Step 8: Probability Aggregation of Areas

In order to derive the desired result, a probability distribution over casualty area associated with spacecraft reentry, we combine the above derived probability distributions. To do this, area bins A^c_l are defined. The first bin (l = 1) corresponds to zero area, corresponding to fragments that completely ablate. Each succeeding bin is incremented by 0.5−1.0 m^2, until all possible casualty areas are included. The probabilities of existence for all fragments $p^{frag}_{e,j,k}$, which have areas lying within bin A^c_l are then summed:

$$p_{e,j}(A^c_l) = \sum_{k=1}^{nfrag} p^{frag}_{e,j,k}(A^c_l < A^c_{e,j,k} \le A^c_{l+1}) \qquad (10)$$

where,

nfrag = maximum number of possible fragments for element e at separation altitude j

$p_{e,j}(\cdot)$ = probability sum of fragments of element e at separation altitude j that are of final casualty area A^c_l

$p^{frag}_{e,j,k}(\cdot)$ = probability of fragment (e, j, k) such that its area is within bin l

Previously calculated for each element was the probability $p^{sep}_{e,j}$ that element e will separate from the spacecraft at altitude j. Thus, for each element the probability of each area bin is given by Eq. 11,

$$p_e(A^c_l) = \sum_{j=1}^{nalt} p_{e,j}(A^c_l)\, p^{sep}_{e,j} \qquad (11)$$

where,

nalt = number of discrete altitudes for which separation was calculated

$p_e(A^c_l)$ = probability of occurrence of casualty area A^c_l owing to element e

Step 9: Element and Total Casualty Areas

Notationally, we define the probability distribution over area for each element $\{p_e(A^c)\}$ as the set of probability-area pairs for each bin l = 1 to *nbins*. There obtains,

$$\{p_e(A^c)\} = [A^c_1, p_e(A^c_1); \ldots; A^c_{nbins}, p_e(A^c_{nbins})] \qquad (12)$$

Then, by adding such probability distributions over all *nelem* elements, the total probability distribution of casualty area is

$$\{p(A^c)\} = \sum_{e=1}^{nelem} \{p_e(A^c)\} \qquad (13)$$

At this point in the work, we believe that individual element distributions $\{p_e(A^c)\}$, may be treated as independent to a good approximation. However, there is a strong correlation among the separation altitudes of each element. If one element separates at a high altitude, for a particular set of parameter values, then other elements will tend to do the same. Therefore, the probability distributions over separation altitude $p^{sep}_{e,j}$ are correlated.

3. DEMONSTRATION OF THE APPROACH

The method is applied to prediction of casualty area for reentry of a Boeing Delta II 2nd stage rocket body. Shown in Fig. 1, a stainless-steel propellant tank forms the main structure of the stage. An aluminum-shell guidance section tops the vehicle, and is attached to the large aluminum miniskirt-truss. The spheres between the aft end of the propellant tank and the forward end of the nozzle hold gaseous helium and nitrogen for the propellant pressurization system. Three of the four titanium spheres are visible in the figure.

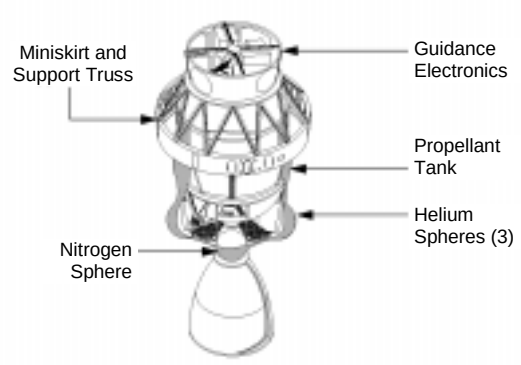

Fig. 1. Schematic of Delta II 2nd Stage
Image courtesy of NASA

The stage was discretized into six element types, corresponding to 31 components: a stainless-steel

cylindrical propellant tank (1), large and small titanium spheres (2 each), aluminum truss members (24), an aluminum miniskirt hoop (1), and an aluminum cylindrical guidance section (1).

Based on data for element material properties and geometric characteristics, bounds and central tendencies were estimated for averaging factor *S*, convective heat transfer coefficient *h*, and emissivity ε, for each element type. Using the Levenberg-Marquardt method [12], coupled with chi-square and Kolmogorov-Smirnov tests [12], the best fit among several distributions (Weibull, log-normal, normal, beta, triangular, and uniform) was used to obtain probability density functions for *S*, *h*, and ε.

Probability distributions over breakup altitude for each element of the 2nd stage were calculated. This required 2000 Latin Hypercube trajectory simulations for all fragments of each element. The result for the stainless-steel propellant tank is shown in Fig. 2. A zero altitude value in Fig. 2 means that, for the combination of parameters selected (*S*, *h*, and ε), the element did not reach the melt temperature and impacted the ground without ablation.

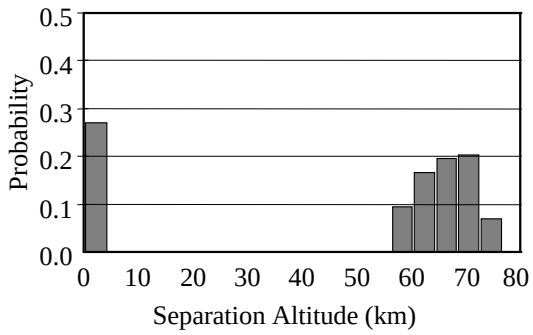

Fig. 2. Stainless-Steel Tank Separation

Consistent with expectation, the aluminum guidance-section was found to demise for all Latin Hypercube trials. This element contributes nothing to the casualty area at ground impact. Analyses outside of the Latin Hypercube framework for the other aluminum components indicated similar results, i.e., none of the assumed components constructed of aluminum survived to ground impact.

The small titanium sphere is well shielded in the trimmed orientation of a reentering Delta II 2nd stage. This coupled with its high melting temperature (1940 K) gave the result that it will survive to ground impact with little or no ablation. Less than 1% of the 2000 simulated trajectories exhibited melting and none of the trials predicted demise.

The large titanium sphere and stainless-steel tank are more interesting. The large sphere location on the reentering vehicle affords it somewhat less shielding than the smaller sphere. About 10% of the simulated trajectories exhibited some ablation with a wide variation in the total amount. These results are consistent with the observation that such spheres impact essentially intact on earth. The stainless-steel tank is essentially not shielded from the aerodynamic heating, once the aluminum structures have separated. About 35% of the simulated trajectories exhibited ablation with approximately 5% of the selected parameter sets exhibiting more than 50% ablation.

Casualty area distribution for the propellant tank is presented in Fig. 3. A surviving and completely intact propellant tank (no ablation) would have a casualty area of 12 m^2. Values in Fig. 3 lower than this correspond to a single tank that has partially ablated. Values larger than 12 m^2 correspond to trajectories in which the tank has fragmented into smaller pieces and these pieces survived the remaining trajectory. Simulations of element fragments accounted for changes in ballistic coefficient, heating radius, and heating area. The total casualty area may be larger when an element fragments for two reasons. First, fragmentation may expose more area projected to the ground. Second, as shown in Eq. 9, each fragment is augmented with the quantity *R* when calculating casualty area. Therefore, element fragmentation may significantly increase casualty area.

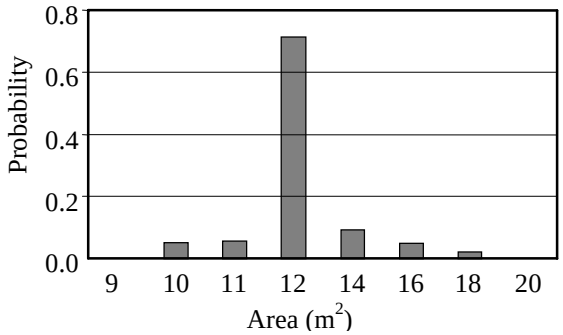

Fig. 3. Stainless-Steel Tank Casualty Area

The total casualty area of a reentering vehicle is the sum of areas of all surviving fragments. For the Delta stage, all element casualty-area distributions (e.g., Fig. 3) are summed. There is no reason to expect strong correlation between casualty-area distributions from different elements. However, both correlated and uncorrelated sums were performed over all elements, with negligible difference in results. The correlated summation is presented in Fig. 4 for total casualty area of a reentering Delta II 2nd stage.

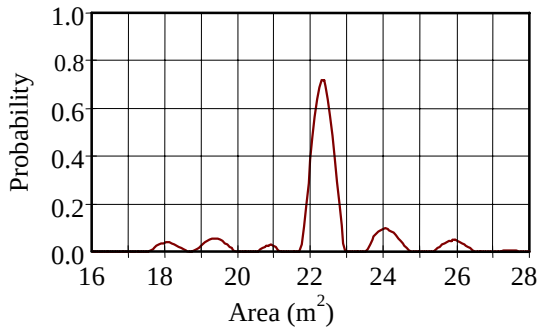

Fig. 4. Total Casualty Area for Delta II 2nd Stage

This curve represents those trajectories for which at least part of the original vehicle elements survived to ground impact. Because only three rather disparate distributions were summed (recall that the aluminum components contributed nothing to the total casualty area), there are not sufficient number of fragments to smooth out the discrete fragment sizes that are clearly visible. The variation enveloping each peak is due to variation in the sensitive parameters (S, h, and ε). The mean area is approximately 22.5 m^2, and represents trajectories over which none of the elements ablated or fragmented. The portion of the curve to the left of the mean represents those simulated trajectories during which one or more elements ablated. The portion of the curve to the right of the mean represents those simulated trajectories during which one or more elements fragmented.

Separate studies revealed that the variation of emissivity ε is much less important to the variation of casualty area than either the averaging factor S or the heat transfer coefficient h. Of these two, the averaging factor is more uncertain than heat transfer coefficient. Immediate further investigation will focus on how to better estimate this parameter.

4. CONCLUSION

A new probabilistic method for obtaining reentry debris area has been presented. This approach accounts for uncertainties in the spacecraft breakup process and quantitatively reveals the downstream influence of these uncertainties. While simple models were used to demonstrate the approach, it is quite amenable to use with higher-fidelity models. Even so, will higher model fidelity significantly decrease the overall uncertainty of results? With availability of this new method, the answer to this important question may now be investigated.

With the initial implementation completed, work now turns to improving specific features of the model. A physically based fragmentation model will be developed using a test case where fragmentation is considered likely (unlike in the Delta II test case). Next, the breakup criterion will account for failure of element attachment points, which may typically occur at earlier times than failure of the bulk element. Refinement of the averaging factor S will include separating out the contributions of geometry, attitude, and aerodynamic shielding for individual study. Future versions of the overall model will include probabilistic treatment of ballistic coefficient and the closely-tied drag coefficient.

This work was funded by The Aerospace Corporation through the Center for Orbital and Reentry Debris Studies, and through the Aerospace Technical Investment Program.

5. REFERENCES

1. Refling, O., Stern, R., and Potz, C., "Review of Orbital Reentry Risk Predictions," ATR-92(2835)-1, The Aerospace Corporation, 15 July 1992.

2. Office of Safety and Mission Assurance (Code Q) and the Johnson Space Center Space Physics Branch, "Guidelines and Assessment Procedures for Limiting Orbital Debris," NASA Safety Standard 1740.14, pp. 7-1–8, August 1995.

3. Fritsche, B., et al., “Spacecraft Disintegration During Uncontrolled Atmospheric Entry,” IAA-99-IAA.6.7.02, 50th International Astronautical Congress, Amsterdam, October 1999.

4. Rochelle, W., et al., “Modeling of Space Debris Reentry Survivability and Comparison of Analytical Methods,” IAA-99-IAA.6.7.03, 50th International Astronautical Congress, Amsterdam, October 1999.

5. Baker, R. L., et al., “Orbital Spacecraft Reentry Breakup”, IAA-99-IAA.6.7.04, 50th International Astronautical Congress, Amsterdam, October 1999.

6. Klinkrad, H., “Evolution of the On-Ground Risk During Uncontrolled Re-entries,” IAA-99-IAA.6.7.05, 50th International Astronautical Congress, Amsterdam, October 1999.

7. Klett, Robert D., "Drag Coefficients and Heating Ratios for Right Circular Cylinders in Free-Molecular and Continuum Flow from Mach 10 to 30," SC-RR-64-2141, Sandia Corporation, December 1964.

8. Cropp, L. O., "Analytical Methods Used in Predicting the Re-Entry Ablation of Spherical and Cylindrical Bodies," SC-RR-65-187, Sandia Corporation, September 1965.

9. Detra, R. W., Kemp., N. H., and Riddell, F. R., “Addendum to ‘Heat Transfer to Satellite Vehicles Re-entering the Atmosphere’,” *Jet Propulsion*, Vol. 27, pp. 1256–7, December 1957.

10. Perini, Luigi L., "Compilation and Correlation of Stagnation Convective Heating Rates on Spherical Bodies," *Journal of Spacecraft and Rockets*, Vol. 12, No. 3, pp. 189–91, March 1975.

11. Baker, R. L. and Nelson, D. A., “Radioisotope Thermoelectric Generator Survivability for Earth Reentries”, *Probabilistic Safety Assessment and Management*, Springer-Verlag, New York, pp. 825–32, 1998.

12. Press, W. H., et al., *Numerical Recipes in FORTRAN: The Art of Scientific Computing*, 2nd ed., Cambridge University Press, Cambridge, 1992.